Insights into the Molecular Mechanism of Inhibition and Drug Resistance for HIV-1 RT with Carbovir Triphosphate[†]

Adrian S. Ray,[‡] Zhenjun Yang,[§] Junxing Shi,[||] Ann Hobbs,[||] Raymond F. Schinazi,[⊥] Chung K. Chu,[§] and Karen S. Anderson*,[‡]

Department of Pharmacology, Yale University School of Medicine, 333 Cedar Street, New Haven, Connecticut 06520-8066, Department of Pharmacology and Biomedical Sciences, College of Pharmacy, The University of Georgia, Athens, Georgia 30602-2352, Pharmasset, Inc., 1860 Montreal Road, Tucker, Georgia 30084, and Laboratory of Biochemical Pharmacology, Emory University/Veterans Affairs Medical Center, 1670 Clairmont Road, Decatur, Georgia 30033

ABSTRACT: Abacavir (1592U89, or Ziagen) is a powerful and selective inhibitor of HIV-1 viral replication that has been approved by the FDA for treatment of acquired immunodeficiency syndrome. Abacavir is metabolized to the active compound carbovir triphosphate (CBVTP). This compound is a guanosine analogue containing a 2′,3′-unsaturation in its planar carbocyclic deoxyribose ring that acts on HIV-1 reverse transcriptase (RT^{WT}) as a molecular target, resulting in chain termination of DNA synthesis. A single amino acid change from methionine 184 to valine in HIV-1 RT (RT^{M184V}) has been observed clinically in response to abacavir treatment. The ability of the natural substrate, dGTP, or CBVTP to be utilized during DNA- and RNA-directed polymerization by RT^{WT} and RT^{M184V} was defined by pre-steady-state kinetic parameters. In the case of RT^{WT}, CBVTP was found to be a surprisingly poor substrate relative to dGTP. In both DNA- and RNA-directed polymerization, a decrease in the efficiency of CBVTP utilization with respect to dGTP was found with RT^{M184V}, suggesting that this mutation confers resistance at the level of CBVMP incorporation. The relatively low incorporation efficiency for RT^{WT} was unanticipated considering earlier studies showing that the triphosphate form of a thymidine nucleoside analogue containing a planar 2′,3′-unsaturated ribose ring, D4TTP, was incorporated with high efficiency relative to the natural substrate, dTTP. The difference may be related to the isosteric replacement of oxygen in the deoxyribose ring with carbon. This hypothesis was tested by synthesizing and evaluating D4GTP (the planar 2′,3′-unsaturated deoxyribose guanosine analogue that is complementary to D4TTP). In contrast to CBVTP, D4GTP was found to be an excellent substrate for RT^{WT} and no resistance was conferred by the M184V mutation, thus providing novel insight into structure−activity relationships for nucleoside-based inhibitors. In this work, we illustrate how an understanding of the molecular mechanism of inhibition and drug resistance led to the discovery of a novel prodrug of D4G. This compound shows promise as a potent antiviral especially with the drug resistant M184V HIV-1 RT that is so often encountered in a clinical setting.

Human immunodeficiency virus (HIV), the causative agent of acquired immunodeficiency syndrome (AIDS),[1] requires reverse transcriptase (RT) to copy its single-stranded RNA genome into a double-stranded DNA copy for integration into the host cell genome. Although almost all aspects of HIV-1's replication cycle have been targeted for therapy (1− 3), a majority of the drugs that have been effective in clinical trials are nucleoside reverse transcriptase inhibitors (NRTIs). However, treatment with NRTIs is limited by their toxicity to the host [often through their interaction with mitochondrial polymerase γ (4−6)] and the ability of the virus to mutate and gain resistance (7). Other factors that affect the ability of these inhibitors to reduce viral replication are uptake, transport, metabolism, and incorporation of the drug. All clinically approved nucleoside analogues lack 3′-hydroxyl groups and are metabolically activated by host cellular kinases to their triphosphate forms. These agents include 3′-azido-3′-deoxythymidine (AZT or Zidovudine), 2′,3′-dide-hydro-3′-deoxythymidine (D4T or Stavudine), (−)-β-L-2′,3′-dideoxy-3′-thiacytidine (3TC or Lamivudine), 2′,3′-dideoxy-

---

* To whom correspondence should be addressed. E-mail: karen.anderson@yale.edu. Phone: (203) 785-4526. Fax: (203) 785-7670.
‡ Yale University School of Medicine.
§ The University of Georgia.
|| Pharmasset, Inc.
⊥ Emory University/Veterans Affairs Medical Center.

[1] Abbreviations: AIDS, acquired immunodeficiency syndrome; HIV-1, human immunodeficiency syndrome type 1; RT, reverse transcriptase; NRTI, nucleoside reverse transcriptase inhibitor; dNMP, 2′-deoxynucleoside 5′-monophosphate; dNTP, 2′-deoxynucleoside 5′-triphosphate; dG, 2′-deoxyguanosine; dC, 2′-deoxycytidine; dT, thymidine; CBV, carbovir; AZT, (+)-β-D-3′-azido-3′-deoxythymidine; (+)-BCH-189, (+)-β-D-2′,3′-dideoxy-3′-thiacytidine; 3TC, (−)-β-L-2′,3′-dideoxy-3′-thiacytidine; D4T, (+)-β-D-2′,3′-didehydro-3′-deoxythymidine; D4G, (+)-β-D-2′,3′-didehydro-2′,3′-dideoxyguanosine; RNase H, ribonuclease H; SAR, structure−activity relationship; WT, wild type; M184V, methionine 184 to valine.
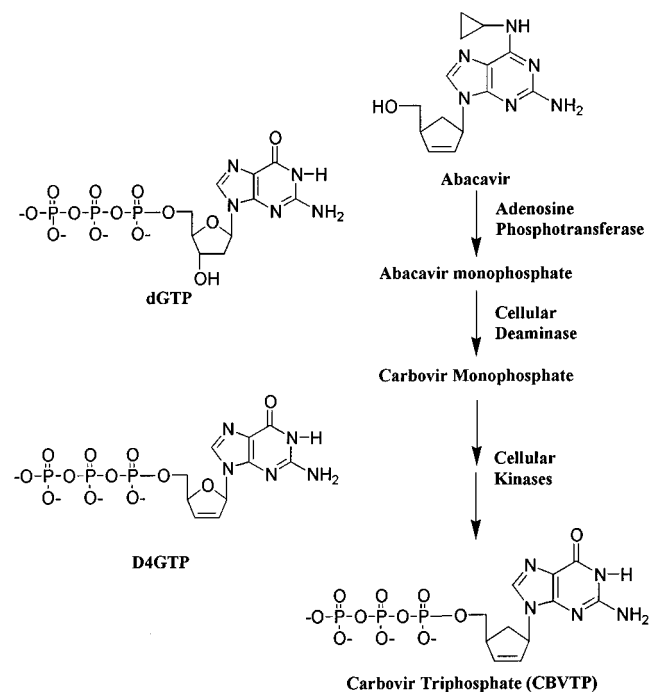
FIGURE 1: Activation of abacavir to the dGTP analogue CBVTP by cellular enzymatic processes (*9, 10*). The structures of dGTP and D4GTP are also shown.

cytidine (ddC or Zalcitabine), and 2′,3′-dideoxyinosine (ddI or Didanosine).

   The structures of the FDA-approved drugs abacavir and D4T are unique because they contain a 2′,3′-unsaturated bond in the deoxyribose ring. Unlike D4T, abacavir contains a novel carbocyclic ring instead of the sugar ring. Abacavir has been shown to be a potent and selective inhibitor of HIV-1 replication (*8*). The metabolic activation of this analogue is unique. It is phosphorylated by adenosine phosphotransferase to a monophosphate and further metabolized in several steps to the triphosphate dGTP analogue (−) carbovir triphosphate (CBVTP; see Figure 1) (*9, 10*). CBVTP is thought to be the agent responsible for antiviral activity (*9, 11−13*). Abacavir has a promising pharmacokinetic profile, due in part to its modified amino group at the 6 position of the purine ring (*8, 14*). Viral resistance to abacavir develops relatively slowly, and the resistance of most mutations is minimal (*8, 15, 16*). When evaluated against human polymerases α, β, and γ, CBVTP was found to be more selective for HIV-1 RT than AZTTP or other 2′,3′-dideoxynucleoside triphosphates, suggesting that it may not cause toxicity through inhibition of host polymerases (*17, 18*).

   Although the resistance profile for abacavir is very good, studies in cell culture and clinical trials have isolated viral mutants in response to prolonged passage or treatment with the drug (*15, 19, 20*). A combination of three mutations in HIV-1 RT has been found in cell culture to be necessary to confer an as high as 11-fold resistance: methionine 184 to valine (M184V), leucine 74 to valine (L74V), and lysine 65 to arginine (K65R) or tyrosine 115 to phenylalanine (Y115F). The first mutation isolated in response to abacavir is the M184V mutation (RT^{M184V}), and this mutation appears to be the cornerstone of higher-level resistance conferred by further mutagenesis. On its own, the M184V mutant virus

has been associated with a 2−4-fold reduction in the virus's susceptibility to abacavir. This same mutant virus has shown a more pronounced 500−1000-fold clinical resistance to 3TC (*21, 22*). Mechanistic studies have shown that RT^{M184V} is 30−140-fold more selective than wild-type RT (RT^{WT}) in distinguishing between dCTP and 3TCTP depending on the primer and template that were used (*23*). These findings show a good correlation between in vitro results and clinical findings.

   While a steady-state kinetic analysis of CBVTP has given a necessary initial inhibitory evaluation (*17, 18, 24*), this approach cannot elucidate the detailed interactions of the drug with RT at the polymerase active site. The reason for the limited scope of steady-state experiments is their inability to resolve kinetic steps masked by the rate-limiting step of a reaction. This point is particularly important with the reaction mechanism of RT. RT follows an ordered reaction pathway (*25*). The first step involves binding of the DNA or RNA substrate to the enzyme to form an E·DNA complex with a dissociation constant (K_d) in the nanomolar range. This step is followed by the binding of a deoxynucleoside triphosphate (dNTP) to form the ternary complex (E·DNA·dNTP). The binding of dNTP is a two-step process with an initial loose complex followed by a tighter binding complex (*26*) as the enzyme undergoes the rate-limiting conformational change for catalysis (k_{pol}) and checks base geometry (*27*) and pairing. Once the conformational change has taken place, the 3′-hydroxyl of the elongating strand attacks the α-phosphate of the dNTP in a rapid chemical step. The rate-limiting step for the reaction (k_{ss}) is the release of the elongated DNA from RT. This is the step being examined during steady-state kinetic analysis.

   Abacavir has been approved for treatment of HIV-1, but no in-depth mechanistic studies have been done on CBVTP and its interactions with HIV-1 RT^{WT} and RT^{M184V}. In the study presented here, we use transient kinetic techniques to gain a better understanding of CBVMP incorporation as well as to provide a broader understanding of structure−activity relationships (SARs) for nucleoside-based inhibitors of HIV-1 RT. Our preliminary results from studies with CBVTP (*28*) prompted the synthesis and kinetic characterization of another nucleoside analogue triphosphate, D4GTP, and allow us to provide novel insight into the structural features of nucleoside analogues that may be important for optimal incorporation efficiency and interaction with HIV-1 RT, the molecular target enzyme. The issues that these experiments were designed to address include (i) differences between the incorporation of dGMP and CBVMP into both primer/template DNA/DNA and DNA/RNA, (ii) the impact of the M184V mutation on HIV-1 RT's ability to distinguish between the two substrates, and (iii) the effect of replacing the carbon in the carbocyclic ring of CBVTP with an oxygen (to make D4GTP) on dNMP incorporation by RT^{WT} and RT^{M184V}. A broader goal of our studies is to attain a better understanding of the kinetic mechanism of incorporation and the contribution of individual residues to this process. The derived kinetic information provides a quantitative basis for comparison of the utilization of CBVTP and D4GTP to the natural substrate (dGTP) by RT^{WT} and RT^{M184V}. Moreover, coupled with previous transient kinetic studies of nucleoside analogue incorporation (*23, 29−34*), a structure−activity relationship (SAR) that correlates structural and stereochem-

ical features of nucleoside analogue drugs with their kinetic and mechanistic behavior toward HIV-1 RT is emerging and should serve as an integral part in future drug design (*35*).

MATERIALS AND METHODS

Purification of HIV-1 RT. RT^{WT} and RT^{M184V} were used for all experiments. The N-terminal histidine-tagged heterodimeric p66/p51 enzymes were purified using clones generously provided by S. Hughes, P. Boyer, and A. Ferris (Frederick Cancer Research and Development Center, Frederick, MD). Purifications were performed as previously described (*30, 36*).

Nucleoside Triphosphates. dGTP was purchased from Pharmacia LKB Biotechnology Inc. The (−)-CBVTP was generously provided by W. B. Parker (Southern Research Institute, Birmingham, AL). The compound was further purified using HPLC utilizing a gradient from 20 to 60% triethylammonium bicarbonate (TEAB) in water and a Pharmacia ion exchange column (mono Q HR 5/5). Its identity was verified using LC−ESI mass spectrometry. The concentration of purified CBVTP was determined using an extinction coefficient ϵ_{253} of 13 260 M^{-1} cm^{-1} (*17*).

D-D4G Synthesis. D4G was synthesized by previously published methods (*37*).

Preparation of D-D4G 5′-Triphosphate. To a solution of D4G (7.5 mg) in (CH$_3$O)$_3$PO (250 μL) at 0 °C was added 2,4,6-collidine (250 μL), and the solution was stirred at 0 °C for 10 min. A solution of POCl$_3$ in (CH$_3$O)$_3$PO (1 M solution, 75 μL) was added, and the reaction solution was stirred at 0 °C for an additional 4 h. Then a solution of bis-(tributylammonium) pyrophosphate in anhydrous DMF (0.5 M solution, 300 μL) and Bu$_3$N (150 μL) were added sequentially. After the mixture had been stirred at room temperature for 30 min, a 0.2 M TEAB solution (2.2 mL) was poured into the above solution and the resulting mixture was stirred at room temperature for 45 min. The solution was filtered, and the filtrate was purified by HPLC [DIONEX NucleoPac PA-100 (9 mm × 250 mm) column; buffer A, 0.05 M TEAB; buffer B, 0.5 M TEAB; flow rate, 7.5 mL/min; gradient, increasing buffer B from 0% at 0 min to 50% at 10 min, and then 100% at 12 min and maintained for 17 min]. Collection and lyophilization of the peak, which had a retention time of 8.5 min, afforded the product as a colorless syrup. The purity of the product, as shown by HPLC [DIONEX NucleoPac PA-100 (4 mm × 250 mm) column; buffer A, 25 mM Tris-HCl (pH 8); buffer B, 0.5 M NaCl in 25 mM Tris-HCl (pH 8); flow rate, 1.5 mL/min; gradient, starting from 100% buffer A, by increasing buffer B from 0% at 1 min to 50% at 15 min, and then 80% at 18 min and maintained until 23 min; retention time, 9.0 min], was >98%. MS (FAB$^-$) m/e 488 ([M − H]$^-$). This compound is very acid labile, and care was taken to keep it in well-buffered, basic conditions. The concentration of D4GTP was determined using the extinction coefficient for dGTP (ϵ_{260} = 11 900 M^{-1} cm^{-1} at pH 7.0).

Oligonucleotides. A 30-mer DNA primer and a 45-mer DNA or RNA template were used (5′-GCCTCGCAGC-CGTCCAACCAACTCAACCTC-3′ and 3′-CGGAGCGTCG-GCAGGTTGGTTGAGTTGGAGCTAGGTTACGGCAGG-5′, respectively).

In the RNA template, the T's are replaced by U's and the underlined sequences represent expected RNase H cleavage

sites (18 and 21 base pairs from the site of incorporation shown in bold italics, respectively). The 30- and 45-mer DNA oligonucleotides that are shown were synthesized on an Applied Biosystems 380A DNA synthesizer (Keck DNA synthesis facility, Yale University, New Haven, CT) and purified using 20% polyacrylamide denaturing gel electrophoresis. The 45-mer RNA oligonucleotide was synthesized and purified by New England Biolabs.

The 30-mer DNA and 45-mer RNA were 5′-^{32}P-labeled with T4 polynucleotide kinase (New England Biolabs) as previously described (*25*). [γ-^{32}P]ATP was purchased from Amersham/Pharmacia. Biospin columns for the removal of excess [γ-^{32}P]ATP were purchased from Bio-Rad.

Annealing of the 30- and 45-mer primer/template DNA/DNA and DNA/RNA was carried out by adding a 1:1.4 molar ratio of purified 30- to 45-mer at 90 °C for 5 min, at 50 °C for 10 min, and on ice for 10 min. The annealed primer and template were then analyzed using 15% nondenaturing polyacrylamide gel electrophoresis to ensure complete annealing. Concentrations of the oligonucleotides were estimated by UV absorbance at 260 nm using the following calculated extinction coefficients: ϵ_{260} = 293 750 M^{-1} cm^{-1} for DNA 30-mer, ϵ_{260} = 491 960 M^{-1} cm^{-1} for DNA 45-mer, and ϵ_{260} = 507 960 M^{-1} cm^{-1} for RNA 45-mer.

Pre-Steady-State Burst and Single-Turnover Experiments. Rapid chemical quench experiments were performed as previously described with a KinTek Instruments model RQF-3 rapid-quench-flow apparatus (*25, 36*).

A pre-steady-state kinetic analysis was used to examine the incorporation of dGMP, CBVMP, and D4GMP into a DNA/DNA or DNA/RNA duplex. A combination of single-turnover and pre-steady-state burst experiments was used to determine the rate dependence on deoxynucleotide concentration. In general for rates of >2 s^{-1}, pre-steady-state burst experiments were used because the incidence of complex kinetics was found to be reduced under these conditions and a more precise rate measurement was possible. Pre-steady-state burst analysis was done with a primer/template concentration 3 times greater than the active enzyme concentration. The reactions were carried out by rapid mixing of a solution containing the preincubated complex of 200 nM (active site concentration) HIV-1 RT (wild type or M184V) and 600 nM 5′-labeled DNA/DNA or DNA/RNA duplex with a solution of 20 mM Mg^{2+} and varying concentrations of dNTP in the presence of 50 mM Tris-HCl and 50 mM NaCl at pH 7.8 and 37 °C. Polymerization was quenched using 0.3 M EDTA at varying time intervals. DNA polymerization and RNA cleavage products were separated using 15% sequencing gel analysis.

Incorporation of CBVMP into a DNA/DNA duplex by HIV-1 RT^{WT} with CBVTP concentrations of <20 μM showed a very shallow burst reflecting a slow rate of incorporation relative to the steady-state rate. Thus, burst experiments were not sufficient for precise measurements of rate. Therefore, single-turnover experiments were necessary to determine observed rate constants at these concentrations. Single-turnover experiments were performed in the same manner described above for a pre-steady-state burst except that enzyme (250 nM final active site concentration) was used in excess of 5′-labeled DNA/DNA duplex (50 nM, final concentration). Single-turnover experiments were also used to study the kinetic behavior of dGMP and D4GMP
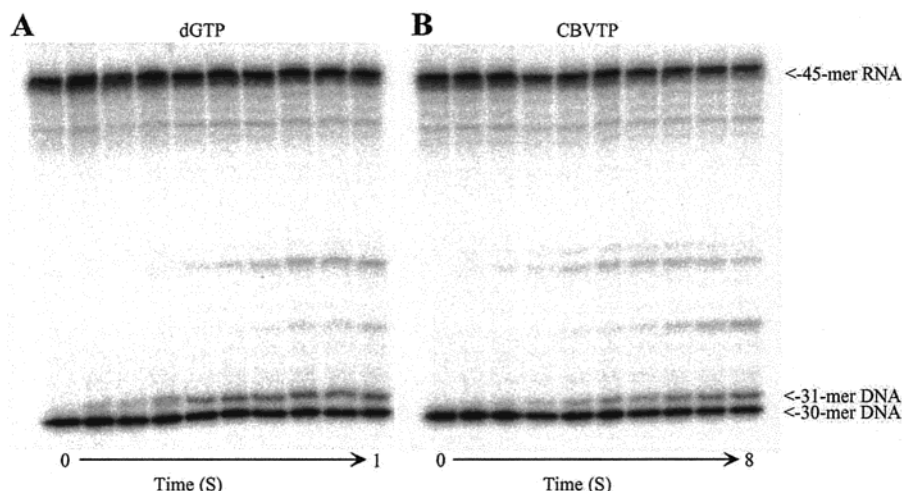
FIGURE 2: Sequencing gel (16%) analysis of a pre-steady-state burst experiment examining the incorporation of dGMP or CBVMP. For each time course, 300 nM DNA/RNA primer/template was preincubated with 100 nM (active site concentration) RT^{WT} and then rapidly mixed with either 40 μM dGTP (A) or 40 μM CBVTP (B) with 10 mM $MgCl_2$ with buffer (all concentrations final, after mixing). The reactions were quenched at the indicated times, and the gels were analyzed by phosphorimaging. The size of the RNA template (45-mer), the DNA primer (30-mer), and the incorporation product (31-mer) are indicated. RNase H cleavage is also observed during incorporation studies with a DNA/RNA primer/template. Upon quantification, it was found that the observed rate constant for cleavage in the presence of dGTP was 3.0 ± 0.3 s^{-1} and in the presence of CBVTP was 0.90 ± 0.04 s^{-1}. These gels are representative of cleavage observed at all the dGTP and CBVTP concentrations that were tested.

incorporation. To test the effect of the order of addition of Mg^{2+}, experiments were carried out under single-turnover conditions, but unlike the normal methodology, 10 mM $MgCl_2$ was incubated with both solutions before mixing. Products were quantified using a Bio-Rad GS525 Molecular Imager (Bio-Rad Laboratories, Inc., Hercules, CA).

Data Analysis. Data were fitted by nonlinear regression using the program KaleidaGraph version 3.09 (Synergy Software, Reading, PA). Results from pre-steady-state burst experiments were fitted to the burst equation [product] = $A[1 - \exp(-k_{obsd}t) + k_{ss}t]$, where A represents the amplitude of the burst which correlates with the concentration of active enzyme, k_{obsd} is the observed first-order rate for dNMP or analogue incorporation, and k_{ss} is the observed steady-state rate constant. Incorporation of dGMP, CBVMP, and D4GMP was found to fit this equation under pre-steady-state burst conditions.

As previously reported, complex kinetics were sometimes encountered during this study under single-turnover conditions (*38*, *39*), and discussion of this kinetic behavior is contained in the text. In most cases, data from single-turnover experiments were biphasic, exhibiting exponential and linear phases, and therefore were fit to a burst equation. The presence of complex kinetic behavior, including a linear phase during dNMP incorporation under single-turnover conditions by HIV-1 RT, has been previously noted by others (*38*, *39*). In the case of dGMP incorporation into a DNA/DNA primer/template under single-turnover conditions, the data showed three distinct phases of incorporation and were found to be most consistent with an equation containing two exponentials followed by a linear phase {[product] = $A_1[1 - \exp(-k_{obsd1}t)] + A_2[1 - \exp(-k_{obsd2}t)] + (A_1 + A_2)k_{ss}t$}. The incorporation of dGMP into a DNA/RNA primer/template was biphasic, including exponential and linear phases. This was also the case for the incorporation of CBVMP into either a DNA/DNA or DNA/RNA primer/template. D4GTP also exhibited complex kinetic behavior under single-turnover conditions. Like the case of dGMP

incorporation into a DNA/DNA primer/template, the incorporation of D4GMP into either a DNA/DNA or DNA/RNA primer/template displayed biphasic kinetic behavior. Therefore, the determination of the kinetic parameters for D4GTP was carried out under burst conditions where the initial, fast phase of elongated product formation was quantitated.

In some cases, the complex kinetic behavior under single-turnover conditions could be altered by preincubating the primer/template enzyme solution with Mg^{2+} (see Figure 4A for dGMP incorporation below). Earlier studies have noted effects of Mg^{2+} preincubation under pre-steady-state burst conditions (*40*). The data for RNase H cleavage of R45 under single-turnover conditions displayed monophasic behavior and were fit to a single-exponential equation.

The dissociation constant (K_d) of dGTP, CBVTP, and D4GTP binding to the binary complex of RT and the primer/template was calculated by fitting observed rate constants at different concentrations of dNTP to the hyperbolic expression $k_{obsd} = (k_{pol}[dNTP])/(K_d + [dNTP])$, where k_{pol} is the maximum first-order rate constant for dNMP incorporation and K_d is the equilibrium dissociation constant for the interaction of dNTP with the E·DNA complex. Reported errors represent the deviation of points from the curve fit generated by KaleidaGraph or were calculated by standard statistical analysis (*41*).

RESULTS

In this comparative study, the kinetic parameters for the addition of dGMP or CBVMP (triphosphate forms shown in Figure 1) into an elongating DNA strand directed by either a DNA or RNA template were determined for HIV-1 RT^{WT} and RT^{M184V}. Pre-steady-state bursts and single-turnover experiments were used to define the maximum rates of incorporation (k_{pol}) and the dissociation constants (K_d). These values were then used to calculate the efficiencies of incorporation (k_{pol}/K_d) to allow for comparison of CBVTP with the natural substrate, dGTP. The efficiencies determined

with each deoxynucleotide with RT^{WT} and RT^{M184V} were used to calculate the selectivity ($efficiency_{dGTP}/efficiency_{CBVTP}$) of each enzyme for the natural substrate, dGTP, relative to the nucleoside analogue, CBVTP. A change in selectivity for RT^{WT} and RT^{M184V} would be anticipated if RT^{M184V} displays drug resistance to a compound and would serve as a basis for comparison with the drug resistance seen in cell culture and clinically. Analysis of the elongation of the DNA/RNA heteroduplex also allowed for the measurement of the rate and the observation of the pattern of RNase H cleavage of the template RNA in the presence of either dGTP or CBVTP. The results obtained for CBVTP prompted the synthesis and study of D4GTP utilization by RT^{WT} and RT^{M184V} for determining the importance of oxygen in the deoxyribose ring. This analysis is part of a broader effort to develop a comprehensive SAR for understanding, at a structural and functional level, the interaction of nucleoside analogues with HIV-1 RT.

Pre-Steady-State Incorporation of dGMP, CBVMP, and D4GMP by HIV-1 RT^{WT}. Previous studies have shown that the overall rate-limiting step for the catalysis of deoxynucleotide incorporation with RT occurs after chemistry (*25*). Under pre-steady-state burst conditions, in which the primer/template is in slight excess over enzyme, a burst of elongated product followed by a linear phase is observed reflecting the overall rate-limiting step (in this case, the release of product). Earlier studies with natural substrates, dATP, dTTP, and dCTP, have revealed bursts of product formation (*25, 29, 30*). Similarly, incorporation of dGMP into both DNA/ DNA homoduplex and DNA/RNA heteroduplex showed a burst of product followed by a slower linear phase.

In the assessment of the incorporation of nucleoside analogues under similar pre-steady-state burst conditions, observation of a burst of product formation indicates a kinetic reaction pathway similar to that of the natural dNTPs. Results from pre-steady-state burst experiments were observed using gel electrophoresis and showed that dGMP (Figure 2A) and CBVMP (Figure 2B) were incorporated in a similar manner, although the rate of CBVMP incorporation was drastically reduced (note the difference in the time scale for panels A and B). Quantitation of these data showed that, like incorporation of the natural substrate, dGMP, a burst of product formation was observed for both homoduplex and heteroduplex elongation with CBVMP, and this was also the case for the incorporation of D4GMP. Representative pre-steady-state burst experiments for dGTP, CBVTP, and D4GTP are shown in panels A, B, and C of Figure 3, respectively.

Single-Turnover Experiments for Evaluating the Incorporation of dGMP, CBVMP, and D4GMP by HIV-1 RT^{WT}. Experiments were performed to study the incorporation of dGMP, CBVMP, and D4GMP under single-turnover conditions (enzyme in excess of primer/template). Since this type of experiment is carried out under pseudo-first-order conditions, the formation of an elongated DNA product would be expected to fit a single-exponential phase as all of the prebound primer/template substrate is converted to product in a single kinetic step. In each case, however, complex kinetic behavior was observed. In most cases, the kinetics were best described by the biphasic formation of product having exponential and linear phases consistent with a pre-steady-state burst equation. In experiments using dGTP,
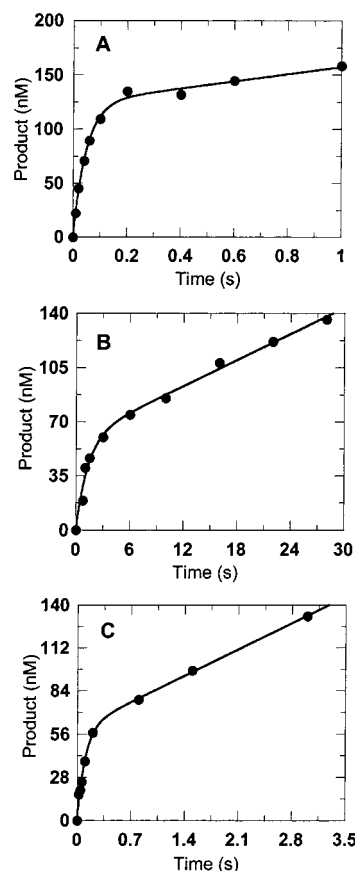

FIGURE 3: Pre-steady-state kinetics of incorporation of various dNMPs into a homoduplex DNA/DNA 30-mer/45-mer primer/ template by HIV-1 RT^{WT} were measured by mixing a preincubated solution of RT^{WT} (100 nM) and 30-mer/45-mer DNA/DNA primer/ template (300 nM) with dNMP and Mg^{2+} (10 mM) under rapid quench conditions. The reactions were quenched at the indicated time points and analyzed by sequencing gel electrophoresis. (A) Incorporation in the presence of 100 μM dGTP. The solid line represents the best fit of the data to a burst equation with an amplitude (A) of 124 ± 4 nM, an observed first-order rate constant for the burst phase (k_{obsd}) of 21 ± 1 s^{-1}, and an observed rate constant for the linear phase (k_{ss}) of 0.27 ± 0.06 s^{-1}. (B) Similar analyses show that 60 μM CBVTP is utilized with an A of 60 ± 5 nM, a k_{obsd} of 0.74 ± 0.13 s^{-1}, and a k_{ss} of 0.05 ± 0.01 s^{-1}. (C) Data showing that 40 μM D4GTP is utilized with an A of 60 ± 3 nM, a k_{obsd} of 9.6 ± 1.1 s^{-1}, and a k_{ss} of 0.41 ± 0.05 s^{-1}.

involving the incorporation of dGMP into a DNA/DNA primer/template under single-turnover conditions, an additional exponential phase was observed as illustrated in Figure 4A (●). Here the data are consistent with two exponential phases ($A_1 = 13 \pm 1$ nM and $k_{obs1} = 19 \pm 3$ s^{-1}; $A_2 = 26 \pm 1$ nM and $k_{obs2} = 1.7 \pm 0.3$ s^{-1}) followed by the steady-state rate ($k_{ss} = 0.24$ s^{-1}). Interestingly, it was found that by altering the reaction conditions so that the enzyme and primer/template were preincubated with Mg^{2+}, before mixing with the dNTP, the second, slower exponential phase was eliminated. Under these conditions, the data for incorporation are most consistent with the burst equation [Figure 4A (○)]. The rate of incorporation during the first exponential phase was increased with Mg^{2+} preincubation (30 ± 3.5 vs 19 ± 3 s^{-1} at 100 μM dGTP). Both dGMP and CBVMP incorporation into a DNA/RNA primer/template was consistent with a pre-steady-state burst of product formation (data not shown). CBVMP incorporation into a DNA/DNA primer/template was also found to fit the pre-
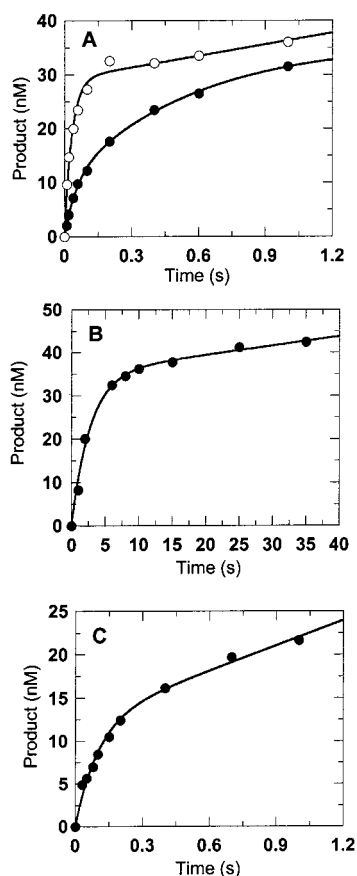
FIGURE 4: Observation of complex kinetics for dNMP incorporation under single-turnover conditions. (A) Effects of Mg^{2+} preincubation on single-turnover kinetics of dGMP incorporation into a DNA/DNA primer/template. Results of a single-turnover experiment where RT^{WT} (250 nM) is in a 5-fold excess over the primer/template (50 nM). The enzyme primer/template was preincubated with 10 mM Mg^{2+} (O) or not (●) and rapidly mixed with a mixture of 100 μM dGTP in the presence of 10 mM Mg^{2+} and buffer. Best fit for the experiment without preincubation (●) was a double exponential plus a line. The first exponential yielded a rate of 19 ± 3 s^{-1} and an amplitude of 10 ± 1 nM. The second exponential had a rate of 1.7 ± 0.3 s^{-1} and an amplitude of 26 ± 1.0 nM. The linear phase was found to be consistent with the steady-state rate of dGMP incorporation (0.24 s^{-1}). The best fit found for data generated with Mg^{2+} preincubation (O) was a single exponential plus a line (burst equation). Where the exponential phase had a rate of 30 ± 4 s^{-1} and an amplitude of 30 ± 1 nM, the linear phase was once again consistent with the steady-state rate (0.24 s^{-1}). (B) The best fit to a single-turnover experiment studying the utilization of 10 μM CBVTP during DNA-directed incorporation by RT^{WT} was found to be a burst equation with an A of 35 ± 2 nM, a k_{obsd} of 0.36 ± 0.04 s^{-1}, and a k_{ss} of 0.0061 ± 0.0022. (C) A single-turnover experiment was performed to study the utilization of 10 μM D4GTP during D4GMP incorporation into a DNA/RNA primer/template by RT^{WT}. The data were found to fit a burst equation with a k_{obsd} of 7.4 ± 0.96 s^{-1} and an amplitude of 13 ± 1.2 nM followed by a slow increase in product formation at a rate of 0.66 ± 0.17 s^{-1} (a rate similar to the steady-state rate of RNA-directed D4GMP incorporation).

steady-state burst equation (Figure 4B) ($A = 35 \pm 2$ nM, $k_{obs} = 0.36 \pm 0.04$ s^{-1}, $k_{ss} = 0.0061 \pm 0.0022$ s^{-1}). Similarly, the incorporation of D4GMP into a DNA/DNA or DNA/RNA primer/template also exhibited biphasic kinetics consistent with exponential and linear phases. A representative time course for D4GMP incorporation into a DNA/RNA primer/template is shown in Figure 4C. The data fit a burst with the following values: $A = 13 \pm 1$ nM, $k_{obs} = 7.4 \pm$

1.0 s^{-1}, and $k_{ss} = 0.61 \pm 0.17$ s^{-1}. It is noteworthy that in experiments involving D4GTP as a substrate, it was found that the amplitude of the exponential phase was lower and may, in part, reflect the much faster steady-state rates observed as compared with that for either dGTP or CBVTP. A single-turnover experiment was carried out, similar to the experiment with dGTP, in which the enzyme DNA/DNA combination was preincubated with Mg^{2+} and an increase in the amplitude of the exponential phase was observed (data not shown).

To provide the most accurate determination of kinetic parameters, the observed rates at varying concentrations of D4GTP were measured by quantitating the initial fast phase of incorporation from pre-steady-state burst experiments by fitting that data to a single-exponential equation.

Determination of the Dissociation Constant and Maximum Rate of Incorporation for dGMP and CBVMP by HIV-1 RT^{WT}. Burst experiments were carried out with various concentrations of dGTP and CBVTP for a DNA/DNA duplex. The difference between the observed burst rate (k_{obsd}) and steady-state rate (k_{ss}) was insufficient for accurate burst analysis at CBVTP concentrations of <20 μM. Consequently, single-turnover experiments were used to derive the observed rate constants at these concentrations.

The interactions between dGTP or CBVTP with the primer/template-bound enzyme were found by plotting the observed rate constants at various concentrations of dGTP or CBVTP and fitting the data to a hyperbolic curve. This curve gave the maximum rate of incorporation of the dNMP (k_{pol}) and the binding affinity for dGTP or CBVTP (K_d). Figure 5A shows the result of this analysis for CBVMP incorporation by RT^{WT} with a DNA/DNA and DNA/RNA duplex (●). Similar curves for dGTP were also constructed for DNA/DNA and DNA/RNA primer/templates (data not shown). The values determined from these curves (k_{pol} and K_d) were used to calculate the efficiency of deoxynucleotide incorporation by dividing k_{pol} by K_d. A summary of these data for dGTP and CBVTP for DNA/DNA and DNA/RNA primer/templates is shown in Table 1.

With a DNA/DNA homoduplex, dGTP proved to be a superior substrate for RT. Its maximum rate of incorporation (k_{pol}) was 24 times faster than that found in the presence of CBVTP (24 ± 1 s^{-1} compared to 1.0 ± 0.06 s^{-1}). dGTP also bound to the enzyme primer/template with a slightly greater affinity (K_d) than CBVTP (14 ± 2 μM compared to 21 ± 3 μM). The efficiency of utilization for dGTP was 1.7 ± 0.3 μM^{-1} s^{-1} which was 30 times greater than that for CBVTP (0.05 ± 0.01 μM^{-1} s^{-1}). Analysis of the data for a DNA/RNA primer/template showed that dGTP was also a better substrate; however, a smaller but significant, 10-fold difference in the incorporation efficiency between dGMP and CBMP for DNA/RNA was noted.

Pre-Steady-State Incorporation of dGMP and CBVMP by M184V HIV-1 RT. Similar to results obtained with RT^{WT}, RT^{M184V} showed a burst of product formation during incorporation of dGMP and CBVMP at all concentrations that were tested and with both primer/templates. This suggests that the mutant RT incorporates these deoxynucleotides by a similar kinetic pathway (data not shown).

Determination of the Dissociation Constant and Maximum Rate of Incorporation of dGMP and CBVMP by M184V HIV-1 RT. Comparison of Selectivity of RT^{M184V} and RT^{WT}.
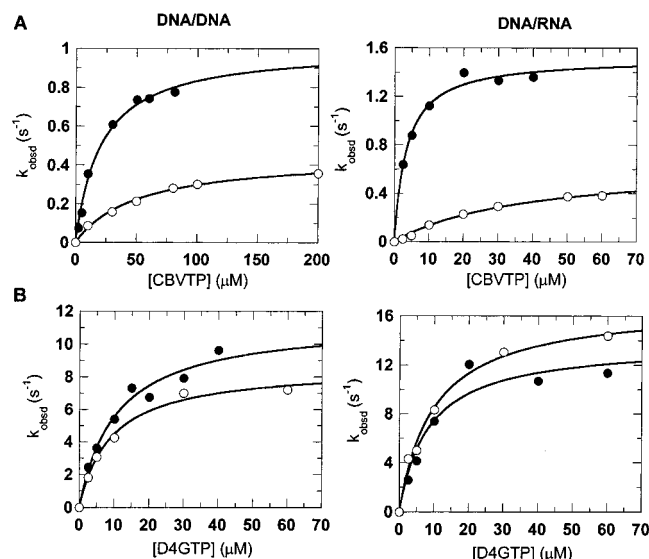
FIGURE 5: Dependence of the first-order rate constant (k_{obsd}) on analogue concentration during both DNA- and RNA-directed synthesis. (A) The observed rates of CBVMP incorporation by RT^{WT} (●) and RT^{M184V} (○) were plotted against CBVTP concentration for both DNA/DNA and DNA/RNA primer/templates. The hyperbolic fit gave a dissociation constant for CBVTP and the primer/template-bound RT (K_d) of 21 ± 3 μM and a maximum rate of incorporation (k_{pol}) of 1.0 ± 0.06 s^{-1} for RT^{WT} and a DNA/DNA primer/template. Similar analysis gave a k_{pol} of 0.45 ± 0.02 s^{-1} and a K_d of 51 ± 5 μM for RT^{M184V} and a DNA/DNA primer/template. Kinetic constants for RT^{WT} and RT^{M184V} during RNA-templated incorporation were equal to 1.5 ± 0.05 and 0.65 ± 0.06 s^{-1} (k_{pol}) and 3.7 ± 0.5 and 38 ± 7 μM (K_d), respectively. (B) The observed rates of D4GMP incorporation by RT^{WT} (●) and RT^{M184V} (○) were plotted against D4GTP concentration for both DNA/DNA and DNA/RNA primer/templates and fit to hyperbolic curves. Kinetic constants for RT^{WT} and RT^{M184V} during DNA-templated incorporation were equal to 11 ± 1 and 8.6 ± 0.4 s^{-1} (k_{pol}) and 11 ± 2 μM and 9.3 ± 1.2 μM (K_d), respectively. Kinetic constants for RT^{WT} and RT^{M184V} during RNA-templated incorporation were equal to 13 ± 0.5 and 17 ± 0.8 s^{-1} (k_{pol}) and 9.5 ± 1.1 and 13 ± 2 μM (K_d), respectively.

Pre-steady-state burst experiments were carried out at various concentrations of dGTP and CBVTP for both DNA/DNA and DNA/RNA primer/templates with RT^{M184V}. Similar to results obtained with RT^{WT}, incorporation in the presence of dGTP was much more rapid than with CBVTP.

The rate dependence on concentration for dGTP or CBVTP with primer/template-bound HIV-1 RT^{M184V} was determined by plotting the observed rates at various concentrations of dGTP or CBVTP and fitting the data to a hyperbolic curve. Figure 5A (○) shows the curve generated for CBVTP with both a homoduplex and a heteroduplex. Similar curves were also generated for dGTP with both primer/templates (data not shown). The k_{pol} and K_d values obtained from these curves were used to calculate the efficiency of deoxynucleotide incorporation by dividing k_{pol} by K_d. A summary of the results of these calculations for dGTP and CBVTP for DNA/DNA and DNA/RNA duplexes with both RT^{WT} and RT^{M184V} is shown in Table 1.

Interestingly, dGTP proved to be an equivalent or slightly better substrate for RT^{M184V}. The efficiencies of incorporation of dGMP into a DNA/DNA primer/template by RT^{WT} and RT^{M184V} were 1.7 ± 0.3 and 2.2 ± 3.3 μM^{-1} s^{-1}, respectively, and similar efficiencies were determined for DNA/

RNA. More importantly, the differences in kinetic parameters between CBVTP and dGTP were larger with the mutant than with wild-type RT and provide a basis for understanding the molecular mechanism of drug resistance. The k_{pol} for dGTP was 78 times faster than that of CBVTP with a homoduplex (35 ± 1 s^{-1} compared to 0.45 ± 0.02 s^{-1}), and accordingly, dGTP bound to the enzyme with a 3-fold tighter dissociation constant (K_d) than CBVTP (16 ± 2 μM compared to 51 ± 5 μM). This corresponds to an efficiency for CBVTP 6-fold lower than that obtained with RT^{WT} (0.009 ± 0.001 μM^{-1} s^{-1} compared to 0.05 ± 0.01 μM^{-1} s^{-1}). There was a 200-fold difference in the efficiency of utilization by RT^{M184V} between dGTP and CBVTP (2.2 ± 0.3 μM^{-1} s^{-1} compared to 0.009 ± 0.001 μM^{-1} s^{-1}). This 200-fold difference is termed the enzyme selectivity for one substrate over another, which is defined as efficiency$_{dGTP}$/efficiency$_{CBVTP}$. RT^{M184V} experienced an almost 7-fold increase in selectivity for dGTP over CBVTP compared to RT^{WT} with a homoduplex.

Results obtained for the heteroduplex were similar to those found with a homoduplex. The efficiency for CBVTP was 25-fold lower than that obtained with RT^{WT} (0.017 ± 0.004 μM^{-1} s^{-1} compared to 0.42 ± 0.06 μM^{-1} s^{-1}). This differential change in selectivity for dGTP relative to CBVTP illustrates that RT^{M184V} has an even greater, 20-fold increase in selectivity over RT^{WT} with a heteroduplex (200 vs 10).

Pre-Steady-State Incorporation of D4GMP by RT^{WT} and RT^{M184V}. Our detailed kinetic analysis with CBVTP indicated that the planar carbocyclic deoxyribose ring resulted in an incorporation efficiency much lower than that of the natural dGTP substrate. This was unanticipated since earlier studies comparing D4TTP and dTTP with HIV-1 RT showed equivalent incorporation efficiencies (*34*) and, based upon the results with CBVTP, lead to the hypothesis that the presence of oxygen in the deoxyribose ring was an important factor in determining incorporation. To directly test this hypothesis, D4GTP (see Figure 1) was synthesized and similar kinetic experiments were carried out as described above.

Determination of the Dissociation Constant and the Maximum Rate of Incorporation for D4GMP by HIV-1 RT^{WT} and RT^{M184V}. Comparison of Selectivity of RT^{M184V} and RT^{WT}. Similar to the analysis of dGTP and CBVTP described above, the rates of incorporation at various concentrations of D4GTP and a DNA/DNA or DNA/RNA primer/template with RT^{WT} and RT^{M184V} were determined and used to find the K_d and k_{pol} for D4GMP incorporation (curves shown in Figure 5B). These values were then used to calculate the efficiency and selectivity for D4GTP utilization by each enzyme as a basis for comparison with dGTP and CBVTP (data summarized in Table 1).

In contrast to the results with CBVTP, the efficiency of utilization of D4GTP was found to be only 2-fold lower than the values obtained for dGTP with both enzymes and primer/template combinations. D4GTP was found to be a $5-100$-fold better substrate than CBVTP depending on the enzyme and primer/template combination. The lack of a difference in the selectivity value between RT^{WT} and RT^{M184V} suggests that RT^{M184V} does not have any advantage over RT^{WT} at selecting dGTP over D4GTP. The marked differences between the incorporation of D4GMP and CBVMP may be explained by the structural features of the protein active site (Figure 6 and Table 2) or deoxynucleotide (Figure 7).

Table 1: Kinetic and Equilibrium Constants for Binding and Incorporation of dGTP, D4GTP, and CBVTP by Wild-Type and M184V HIV-1 RT

primer/template	RT	dNTP	k_{pol} (s^{-1})	K_d (μM)	efficiency[a] (s^{-1} μM^{-1})	selectivity[a,b]
DNA/DNA	RT^{WT}	dGTP	24 ± 1	14 ± 2	1.7 ± 0.3	–
		D4GTP	11 ± 1	11 ± 2	1.1 ± 0.3	2
		CBVTP	1.0 ± 0.1	21 ± 3	0.05 ± 0.01	30
	RT^{M184V}	dGTP	35 ± 1	16 ± 2	2.2 ± 0.3	–
		D4GTP	8.6 ± 0.4	9.3 ± 1.2	0.93 ± 0.13	2
		CBVTP	0.45 ± 0.02	51 ± 5	0.009 ± 0.001	200
DNA/RNA	RT^{WT}	dGTP	35 ± 2	11 ± 2	3.1 ± 0.6	–
		D4GTP	13 ± 0.5	9.5 ± 1.1	1.4 ± 0.2	2
		CBVTP	1.5 ± 0.1	3.7 ± 0.5	0.42 ± 0.06	10
	RT^{M184V}	dGTP	120 ± 13	42 ± 10	2.9 ± 0.8	–
		D4GTP	17 ± 1	13 ± 2	1.7 ± 0.3	2
		CBVTP	0.65 ± 0.06	38 ± 7	0.017 ± 0.004	200

[a] Values for dGTP and CBVTP previously reported in association with a poster presentation (*28*). [b] Selectivity = efficiency$_{dGTP}$/efficiency$_{analogue}$.
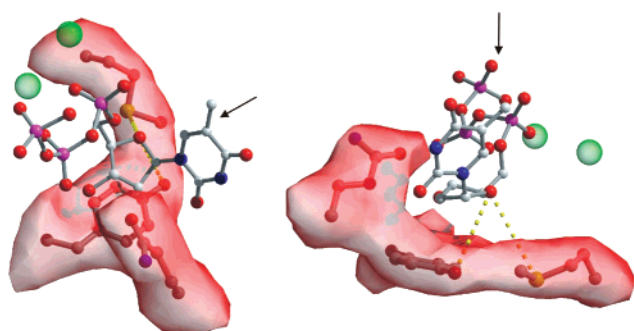

FIGURE 6: Possible interactions for the deoxyribose oxygen in the RT active site. Structural picture generated from the crystal structure of the ternary complex of HIV-1 RT, primer/template, and dTTP (*54*). A solvent accessible contoured surface surrounds RT active site residues Y115, Q151, and M184 and was produced using the program Volumes (R. Esnouf, Oxford, U.K.). Potential interactions between Y115 (4.53 Å) or M184 (4.66 Å) and the deoxyribose oxygen depicted from two different angles. Arrows are used to help orient the viewer and show the angle of observation in the opposite panel. This figure was produced using Bobscript (*72*) and Raster3D (*73*).

Table 2: Proximity of the Oxygens of Steric Gate Amino Acid Side Chains and the Ribose Ring Oxygens in a Wide Variety of DNA Polymerases

polymerase family	polymerase	steric gate amino acid	O–O distance[a] (Å)	ref
reverse transcriptase family A (Pol 1)	HIV-1 RT	Tyr	4.53	*54* (1RTD)
	T7 DNA Pol	Glu	3.72	*55* (1T7P)
	Klentaq Pol I	Glu	3.31	*57* (1QSS)
family B	RB69	Tyr	4.86	*56* (1IG9)
family X	Pol β	Tyr	3.86	*60* (1BPY)

[a] Distance between the ribose oxygen and the oxygen present in the amino acid side chain of the steric gate.

RNase H Cleavage in the Presence of dGTP, CBVTP, and D4GTP. It has been shown that rates of polymerization and RNase H cleavage are independent and that the two active sites lie between 18 and 21 bases apart on the template strand (*25, 36*). Previous work has illustrated that altered dNTP binding at the polymerase active site can effect the rate and pattern of cleavage at the RNase H site (*30*). The R45 template was 5′-^{32}P-labeled in experiments utilizing a heteroduplex to facilitate analysis of the rate and pattern of RNAse H cleavage. Although rates of polymerization for the heteroduplex varied between different concentrations of dGTP and CBVTP with HIV-1 RT^{WT} (between 0.64 and 1.4
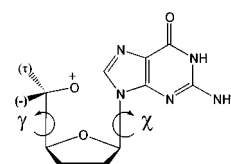

FIGURE 7: Important deoxynucleotide structural features to be considered for nucleoside analogues with a planar dideoxyribose ring conformation. Ring torsion angles γ and χ are labeled. Torsion angle γ reflects the position of the 5′-oxygen and torsion angle χ the base. Different values of γ lead to three general positions of the 5′-oxygen (+, −, and τ). The 5′-oxygen is depicted in the γ^+ position.

s^{-1} for CBVTP and between 7.7 and 27 s^{-1} for dGTP), the rate of RNase cleavage was relatively consistent for each. A representative time course of the gel electrophoresis for CBVTP and dGTP (both at 40 μM) is shown in Figure 2. Both show a similar cleavage pattern with products of 36 and 33 bases. The rate of RNase H cleavage in the presence of CBVTP was found to be 3 times lower than in the presence of dGTP (0.9 s^{-1} compared to 3 s^{-1}). D4GTP also exhibited a slightly slower rate of RNase H cleavage with no difference in pattern when compared to that of dGTP (data not shown). Similar results were obtained when analyzing cleavage products formed during incorporation of dGMP, CBVMP, and D4GMP by RT^{M184V} (data not shown).

DISCUSSION

In this paper, we have examined the transient kinetics for the incorporation of dGMP and CBVMP into homo- and heteroduplex primer/templates catalyzed by RT^{WT} and RT^{M184V}. Subsequent synthesis and evaluation of D4GTP was then used to gain a better understanding of the HIV-1 RT active site and structural features that govern efficient incorporation of nucleoside analogues. Our ultimate goal is to use this mechanistic analysis to build a comprehensive SAR for the interaction of these analogues with wild-type and drug-resistant mutant forms of HIV-1 RT. This information may impact the design of novel nucleoside analogues that are incorporated more efficiently and are less susceptible to developing drug resistance.

Observation of Complex Kinetics under Single-Turnover Conditions by HIV-1 RT. During the course of our studies with these guanosine analogues, upon examination of the incorporation kinetics of RT^{WT} and RT^{M184V} under single-turnover conditions, the data did not fit with the anticipated

single-exponential under pseudo-first-order conditions. In all cases under single-turnover conditions, a slow linear phase of primer elongation was observed after faster initial exponential behavior (Figure 4A−C). This has been previously noted by others and suggested to be due to RT's poor ability to align itself at the 3′-hydroxyl of the elongating chain (*38, 39*). It is also possible that inactive enzyme may sequester the substrate during the initial round of synthesis, contributing to the observation of the linear phase. This possibility cannot be ruled out since the active site concentrations of purified RT are sometimes low (often around 30%). In either case, the rate of incorporation observed during the first exponential phase of incorporation should represent the maximum rate of catalysis (k_{pol}) without compromising the kinetic analysis.

In addition, dGMP was found to be incorporated by RT^{WT} during single-turnover experiments looking at a DNA/DNA primer/template by a process that includes two exponential processes [Figure 4A (●)]. This type of behavior has been seen with all natural dNTPs under single-turnover conditions during the elongation of a DNA/DNA primer/template (data not shown). A previous report observed these kinetics and attributed them to different binding interactions between RT and its primer/template (*39*). Interestingly, no double-exponential behavior could be detected for dGTP when incorporation was studied using pre-steady-state burst conditions. This may suggest that there is a preferential binding of substrate in the most catalytically competent complex when there is an excess of primer/template. Another possible explanation for the observed kinetics is that the binding of the primer/template was rate-limiting; however, experiments conducted at higher enzyme concentrations did not result in higher rates. Moreover, this explanation is less plausible when considering that, under all experimental conditions, the concentrations of the enzyme and primer/template were approximately 1 order of magnitude higher than the binding constant of the enzyme for the primer/template [around 15 nM (*42*)].

To study the role of Mg^{2+} in the complex kinetics observed for dGMP incorporation into a DNA/DNA primer/template under single-turnover conditions, Mg^{2+} was preincubated with the enzyme and primer/template. Using these experimental conditions, the second, slower exponential phase disappeared and an increase in the exponential rate of dGMP incorporation into the primer/template was noted as well. However, no change was detected in the linear phase discussed above [Figure 4A (○)]. This suggests that Mg^{2+} plays an important role in determining the catalytic competence of the enzyme during DNA-directed incorporation. The increase in the rate of incorporation also suggests that the preferred order of binding for RT is Mg^{2+} prior to dNTP. The effect of Mg^{2+} preincubation on RNA-templated incorporation cannot be determined because the associated metal-dependent RNase H activity would slowly degrade the template. Additional studies are required to define the parameters that are responsible for the complex reaction kinetics observed under single-turnover conditions and the role that Mg^{2+} may play in modulating binding or catalysis.

RNA- versus DNA-Dependent Polymerization. A complete study of dGTP or CBVTP concentration dependence on the observed rate of incorporation (k_{obsd}) with mutant and wild-type HIV-1 RT provided measurements of the dissociation constant for each with the E·DNA complex (K_d), the maximum rate of incorporation into the 30-mer primer (k_{pol}), and the efficiency of incorporation (k_{pol}/K_d). In accord with previous studies on the incorporation of dCMP and dTMP and some of their nucleoside analogues, the maximum rates of incorporation were faster with DNA/RNA than with DNA/DNA (*23, 30, 31, 34, 36*). The rate obtained for dGMP incorporation into DNA/RNA by HIV-1 RT^{M184V} (120 s^{-1}) is the fastest rate that has been measured for dNMP incorporation by HIV-1 RT and is an illustration of the dramatic changes this mutation causes in the enzyme reaction kinetics. This rate is only 2−3-fold lower than rates measured with bacteriophages T7 and T4 DNA polymerases (*43, 44*). However, the weak K_d obtained for dGTP with RT^{M184V} (42 μM) causes the efficiency to be 1 order of magnitude lower than values obtained with these other polymerases and consistent with efficiencies obtained with RT^{WT}.

An increased maximum rate of incorporation and affinity for the E·DNA complex of dGTP and CBVTP with RT^{WT} and a RNA template defines a higher efficiency (k_{pol}/K_d) for each with the heteroduplex than with the homoduplex. dGTP showed a 2-fold increase in efficiency during RNA-directed polymerization versus DNA-directed polymerization. CBVTP showed an 8-fold increase in efficiency with a DNA/RNA primer/template with respect to a DNA/DNA primer/template. This differential increase in efficiency for dGTP and CBVTP reflects a 3-fold decrease in selectivity (efficiency$_{dGTP}$/efficiency$_{CBVTP}$) for RNA-directed versus DNA-directed incorporation of dGMP over CBVMP. This result is in contrast to those with other nucleoside analogues where RT has been shown to be more likely to incorporate a chain terminator during DNA-templated polymerization (*45, 46*). This difference may be an illustration of the extreme effect the carbocyclic ring elicits on the kinetics of CBVMP incorporation.

Effects of a Carbocyclic Ring on Incorporation Efficiency and RNase H Cleavage. Previous studies with D4TTP have shown it to be the most effective analogue at mimicking its natural dNTP (dTTP) in the HIV-1 RT^{WT} active site (*34*). The substitution of the oxygen in the unsaturated dideoxyribose ring with a methylene group, as found in the carbocyclic ring present in CBVTP, seemed to be a minimal perturbation, and therefore, the marked impact this isosteric replacement had on the incorporation kinetics for this analogue was surprising. Only minor changes in binding were observed with RT^{WT}; the K_d of CBVTP was less than 2-fold greater than that for dGTP with a homoduplex, and the affinity was 3-fold lower than that for dGTP with a heteroduplex. This finding is supported by a computer modeling study comparing NRTIs in their lowest-energy state conformation. This study predicted that CBVTP would bind well to HIV-1 RT's active site (*47*). Our kinetic analysis showed that the primary effect of the carbocyclic ring of CBVTP was reflected in the maximum rate of incorporation (k_{pol}) into a homo- and heteroduplex, which was found to be reduced 23−24-fold relative to the rate of dGMP incorporation with RT^{WT}. Furthermore, steady-state studies of the triphosphate of the carbocyclic analogue of 2′-deoxyguanosine triphosphate (CdGTP) found that it was a poor substrate for HIV-1 RT (*48*) and CdG showed no anti-HIV-1 activity in cell culture despite its conversion to the potentially active triphosphate, CdGTP (*49*). Also, further

evidence that CBVTP is a poor substrate for DNA polymerases can be obtained from a recent transient kinetic study on mitochondrial polymerase γ where it was found that CBVTP was the worst substrate in a panel of FDA-approved nucleoside analogue triphosphates (6).

The reduced ability to be utilized may reflect the fact that CBVTP cannot assume a favorable conformation like that adopted by the conventional deoxyribose ring during catalysis. Studies with D4TTP have shown that the 2′,3′-unsaturation does not have a negative effect on D4TMP incorporation (34). It is improbable that dGTP analogues function differently than dTTP analogues and likely that the replacement of the dideoxyribose oxygen with the methylene carbon is the structural moiety that is responsible for the decreased rate of incorporation. Perturbations in the 2′,3′-dideoxyribose ring present in (+)-BCH-189TP and 3TCTP caused by the presence of a sulfur in place of the 3′-carbon caused similar kinetic consequences for these compounds (30). It is possible that preferred conformations in the sugar ring may be required for high rates of incorporation that are precluded by the replacement of the oxygen with a carbon (as in CBV), a change in stereochemistry (as in 3TC), or the introduction of a sulfur atom [(+)-BCH-189 and 3TC]. It is also possible that these changes affect electrostatic or steric interactions with the RT active site which are responsible for higher rates of catalysis (see the structural discussion that follows).

Studies with 3TCTP showed an altered binding of the drug in both the kinetic data for incorporation and the pattern and rate of RNase H cleavage (30). In the study presented here, RNase H cleavage was evaluated to determine if there were any altered interactions between CBVTP and the E·DNA complex at the polymerase active site that may be sufficient to affect the distant RNase H active site. The pattern for cleavage was very similar between dGTP and CBVTP (Figure 2). However, the rate was found to be 3-fold higher in the presence of dGTP than in the presence of CBVTP with both RT^M184V and RT^WT. Subsequent experiments with D4GTP also showed a similar reduction in the rate of cleavage (data not shown). These reduced cleavage rates are similar to the difference in the rate seen in the presence of dCTP and 3TCTP (30). This difference in rate may reflect a perturbation in the ternary complex in the presence of 3TCTP, CBVTP, and D4GTP. Further kinetic experimentation and a better structural understanding of HIV-1 RT are required to define the significance of these types of changes in RNase H cleavage.

Increase in Selectivity of dGTP over CBVTP by RT^M184V Compared with RT^WT. Insights into the Molecular Mechanism of Drug Resistance. Previous transient kinetic studies with 3TCTP have shown a 140-fold increase in selectivity by RT^M184V over RT^WT in DNA-directed polymerization and a smaller 34-fold increase in selectivity in RNA-directed polymerization (23). The M184V mutant exhibited a less dramatic increase in selectivity against CBVTP (a 7-fold increase for DNA-directed polymerization and a 20-fold increase for RNA-directed polymerization). The higher level of resistance conferred during RNA-directed polymerization shows that RT^M184V can compensate for RT^WT's enhanced sensitivity to CBVMP chain termination during RNA-directed polymerization. The increase in selectivity obtained by the enzyme in RNA- and DNA-directed polymerization is a consequence of a decrease in both the affinity for CBVTP

(K_d) and the maximum rate of incorporation of the analogue (k_{pol}). The smaller change in selectivity by the mutant enzyme for CBVTP when compared to that for 3TCTP is consistent with the clinical findings that the M184V mutation only imparts a low level (2−4-fold) of resistance to abacavir (19, 20) while a 500−1000-fold resistance is observed for 3TC (21, 22). The amount of resistance to incorporation found in this study is greater than that found in cell culture or in clinical studies (15, 19, 20). This slight discrepancy may be due to inherent differences in the measurements, or the smaller amount of resistance recognized in vivo may reflect a decrease in the fitness of the virus due to the presence of the M184V mutation (50).

Importance of the Sugar Ring Rather Than Base Identity in Analogue Incorporation by HIV-1 RT. Previous kinetic studies with D4TTP showed that D4TMP was as efficiently incorporated as dTMP (34, 51). Similar to this result, elongation in the presence of D4GTP was found to be only 2-fold less efficient than in the presence of dGTP. RT with the M184V mutation was also found not to be resistant to D4GTP. While D4TTP has not been tested against RT^M184V in a transient kinetic study, this mutation has never been associated with D4T resistance in vivo or in vitro (52). These results suggest that the 2′,3′-dideoxyribose ring of the analogue is an important factor in governing its incorporation and the base may play a less prominent role in determining incorporation efficiency or resistance. The differences between CBVTP's and D4GTP's utilization and resistance found in this study show that RT is exquisitely sensitive at detecting small changes in the 2′,3′-deoxyribose ring.

Structural Basis for the Large Differences in Incorporation in the Presence of CBVTP and D4GTP by RT^WT and RT^M184V. CBVTP was found to be 30-fold less efficiently utilized than dGTP by RT^WT, and the mutation of methionine 184 to valine increased this difference to 200-fold. This is in stark contrast to D4GTP, which is utilized with efficiencies very similar to that of dGTP and is *not* selected against by the M184V mutation. The differences in these two compounds, which only differ in the replacement of a carbon with an oxygen, suggest that some attribute of the RT active site or some structural feature of the deoxynucleotide analogues must be markedly affected by this change.

Two residues in the RT active site that could potentially interact with the oxygen in the 2′-deoxyribose ring are tyrosine 115 and methionine 184. Tyrosine 115 is the "steric gate" of RT that is partially responsible for excluding the binding of the 2′-hydroxyl of an RNA nucleotide (53). This residue also has important stacking interactions with the deoxyribose ring (54). Structural analyses of ternary complexes of a wide variety of DNA polymerases from different polymerase families (54−60) and the position and identity of their steric gates show that this residue can normally serve as a hydrogen bond donor [the presence of phenylalanine in the active sites of Moloney murine leukemia virus RT (53) and some DinB homologues (61, 62) are two exceptions]. In almost every case, not only is this residue a hydrogen bond donor, but the position of this donor also is in the proximity of the oxygen of the deoxyribose ring (Table 2). This is especially true of Pol I family members from bacteria and bacteriophages (63) where the residue is a glutamate and in the available ternary crystal structures, within 4 Å of the deoxyribose oxygen (55−59). The distance in RT is

slightly longer than a normal hydrogen bond, but the crystal structure is a static view of a dynamic active site and may not be of sufficient resolution to allow solid conclusions to be drawn (*54*). The sulfur of residue M184 is also in the proximity of and could potentially interact with the ribose ring (possible interactions are illustrated in Figure 6).

The polar attributes of Y115 and M184 may also repel the more hydrophobic carbocyclic ring present in CBVTP. While the repulsion of these residues might serve to weaken the binding of the analogue, CBVTP binding over the aromatic ring of Y115 could allow for a very tight hydrophobic and possible $\pi-\pi$ orbital stacking interaction between the sugar ring and this residue. These two opposing forces may cause CBVTP to bind very differently depending on its positioning in the presence of different substrates or mutant forms of the enzyme. This may explain CBVTP's relatively loose binding during DNA/DNA incorporation by RT^{WT} and, conversely, its tight relative binding during DNA/RNA incorporation by RT^{WT}.

The resistance caused by the M184V mutation may also be associated with the position of the RT active site. It is unlikely that resistance to CBVTP is conferred by steric hindrance due to the presence of the β-branched amino acid [as is the case with the L-isomer 3TC (*23, 64*)] because of the large distance between the dideoxyribose ring of an analogue that mimics the natural D-isomer orientation and this amino acid. However, methionine 184 has many important contacts in the RT active site. This residue is at a reasonable distance to interact in a hydrogen bond with Y115, which has already been discussed as a possible important residue in the active site for CBVMP incorporation. Further evidence for the intimate nature of the contact of Y115 with the incoming dNTP is suggested by the observation that a conservative mutation to phenylalanine (Y115F) is found in response to abacavir in cell culture, and evaluation by steady-state kinetic analysis shows a slight resistance (*15, 65*). M184 also makes steric contact with the primer/template, and loss of this interaction may change the position of the active site. If the change from valine to methionine in M184V caused a subtle alteration in the deoxynucleotide sugar binding site into a slightly more hydrophilic position, this could explain the drop in affinity seen for CBVTP with the mutant enzyme.

Another possible reason for the difference in incorporation and resistance between CBVTP and D4GTP is the structure of the dideoxyribose ring of the analogue. While in both cases the dideoxyribose rings of these compounds are locked in planar conformations that probably have only limited flexibility [this is illustrated by the crystal structure of D4T (*66*)], the different rings may have effects on the rotational conformations effecting the positions of the 5′-oxygen and the guanine base (Figure 7). Studies on adenosine deaminase have shown that the ability of nucleoside analogues to obtain a γ^+ conformation is critical for determining their efficiency as a substrate, and suggest that most analogues can easily adjust the χ torsion angle to favorably position the base (*67, 68*). dTTP is also found to be in the γ^+ position in the HIV-1 RT active site (*54*). The γ^+ position places the 5′-oxygen directly above the deoxyribose ring. In the case of CBVTP, this might be unfavorable because of increased hydrophobicity of its dideoxyribose ring. If CBVTP was limited in its ability to adopt the γ^+ torsion angle, this would lead to a difference in the triphoshate positioning. Indeed, a differ-

ence in the position of the α-phosphate could explain the slower rate of incorporation of CBVMP relative to those of dGMP and D4GMP. A mutation at position 65 (lysine 65 to arginine) has also been noted in response to abacavir treatment (*15, 19*) and is responsible for the 3-fold resistance to abacavir in cell culture (*15*). Lysine 65 is in contact with the γ-phosphate, and a mutation at this position may sense differences in analogues at this phosphate. This mutant has not been reported in response to D4T (*69*) and does not show resistance to D4T in cell culture (*15*). Taken together, these findings may also suggest differences in the phosphate position of D4GTP and CBVTP, which could be due to the γ torsion angle. As discussed, the M184V mutation may also alter the dNTP binding site and exaggerate differences in dideoxyribose structure.

Conclusions. The transient kinetic study of CBVTP as a substrate for RT and resistance to the incorporation of CBVMP caused by the M184V mutation have yielded many insights into not only the incorporation of this deoxynucleotide analogue but also the mechanism of incorporation of natural dNMPs. Complex kinetics observed during deoxynucleotide incorporation suggest that the preferred order of binding is Mg^{2+} before the dNTP, implying that Mg^{2+} plays an important role in the proper positioning of substrates for effective catalysis. While the identity of the base had little effect on the efficiency of incorporation, RT was found to be exquisitely sensitive to changes in the deoxyribose ring. The sensitivity to substitutions in the deoxyribose ring may be due to key polymerase active site residues and effects on deoxynucleotide structure. A combination of these factors is probably responsible for the poor incorporation of CBVMP and resistance conferred to CBVTP by the M184V mutation.

An Understanding of SAR for Nucleoside-Based Analogues Targeting HIV-1 RT and Implications for Drug Design. As discussed above, the mechanistic studies reveal that analogues containing an unsaturated deoxyribose ring as in D4TTP and D4GTP are very efficiently incorporated into DNA by HIV-1 RT (*34, 51*) and, accordingly, are difficult for the enzyme to distinguish from the respective natural substrates, dTTP and dGTP. Consequently, a low selectivity or ability of HIV-1 RT to distinguish between natural dNTP and substrate analogue suggests that it may be more difficult for the virus to develop drug resistance through mutations in RT. Cell culture and clinical data support this suggestion in the case of D4T (*15, 70*).

Having established that D4GTP was a good substrate for RT, we were surprised to find an early literature report indicating that the corresponding nucleoside had no antiviral activity in cell culture (*37*). The lack of antiviral activity may be due to a number of factors, including metabolic activation, stability, or transport. Prompted by our mechanistic studies, we have recently re-examined D4G in an attempt to understand why the compound is inactive. Our studies have found that the nucleoside was acid labile, and moreover, when tested under carefully buffered conditions, D4G exhibits excellent antiviral activity (*71*). Furthermore, we have synthesized and tested a prodrug form of D4G containing a cyclopropylamine substitution in the 6 position of the guanine ring which has improved acid stability and retains good antiviral activity against HIV-1 (*71*).

In summary, this work illustrates the general importance of mechanistic studies and how the information they provide

can impact the design of novel nucleoside analogues. More specifically, this study exemplifies the value of understanding the mechanism and SAR for HIV-1 RT. In this example, there is a very clear link between translating the molecular mechanism of inhibition and drug resistance to observations in the clinic. These mechanistic insights have aided in the design, synthesis, and discovery of a new compound that has promise as a potent antiviral especially with the drug resistant M184V HIV-1 RT that is so often encountered in a clinical setting.

NOTE ADDED AFTER ASAP POSTING

This article was inadvertently posted ASAP on 03/27/02 before final corrections were made. In Table 2, RB69 is now correctly identified as a family B polymerase. The correct version was posted 04/16/02.

REFERENCES

1. De Clercq, E. (1995) *J. Med. Chem. 38*, 2491−2517.
2. De Clercq, E. (1997) *Clin. Microbiol. Rev. 10*, 674−693.
3. Mitsuya, H., Yarchoan, R., Kageyama, S., and Broder, S. (1991) *FASEB J. 5*, 2369−2381.
4. Parker, W. B., and Cheng, Y.-C. (1994) *J. NIH Res. 6*, 57−61.
5. Martin, J. L., Brown, C. E., Matthews-Davis, N., and Reardon, J. E. (1994) *Antimicrob. Agents Chemother. 38*, 2743−2749.
6. Johnson, A. A., Ray, A. S., Hanes, J. W., Suo, Z., Colacino, J. M., Anderson, K. S., and Johnson, K. A. (2001) *J. Biol. Chem. 276*, 40847−40857.
7. Larder, B. A. (1994) *J. Gen. Virol. 75*, 951−957.
8. Daluge, S. M., Good, S. S., Faletto, M. B., Miller, W. H., St. Clair, M. H., Boone, L. R., Tisdale, M., Parry, N. R., Reardon, J. E., Dornsife, R. E., Averett, D. R., and Krenitsky, T. A. (1997) *Antimicrob. Agents Chemother. 41*, 1082−1093.
9. Faletto, M. B., Miller, W. H., Garvey, E. P., St. Clair, M. H., Daluge, S. M., and Good, S. S. (1997) *Antimicrob. Agents Chemother. 41*, 1099−1107.
10. Parker, W. B., Shaddix, S. C., Bowdon, B. J., Rose, L. M., Vince, R., Shannon, W. M., and Bennett, L. L., Jr. (1993) *Antimicrob. Agents Chemother. 37*, 1004−1009.
11. Vince, R., Hua, M., Brownell, J., Daluge, S. M., Lee, F. C., Shannon, W. M., Lavelle, G. C., Qualls, J., Weislow, O. S., Kiser, R., Canonico, P. G., Schultz, R. H., Narayanan, V. L., Mayo, J. G., Shoemaker, R. H., and Boyd, M. R. (1988) *Biochem. Biophys. Res. Commun. 156*, 1046−1053.
12. Vince, R., and Hua, M. (1990) *J. Med. Chem. 37*, 17−21.
13. Wolbach, J., and Capoccia, K. (1999) *Nurse Pract. 24*, 81−82, 87−90, 92.
14. Foster, R. H., and Faulds, D. (1998) *Drugs 55*, 729−738.
15. Tisdale, M., Alnadaf, T., and Cousens, D. (1997) *Antimicrob. Agents Chemother. 41*, 1094−1098.
16. Mellors, J. W., Hertogs, K., Peeters, F., et al. (1998) in *Fifth Conference on Retroviruses and Opportunistic Infections*, Chicago, IL.
17. White, E. L., Parker, W. B., Macy, L. J., Shaddix, S. C., McCaleb, G., Secrist, J. A., III, Vince, R., and Shannon, W. M. (1989) *Biochem. Biophys. Res. Commun. 161*, 393−398.
18. Parker, W. B., White, E. L., Shaddix, S. C., Ross, L. J., Buckheit, R. W., Germany, J. M., Secrist, J. A., Vince, R., and Shannon, W. M. (1991) *J. Biol. Chem. 266*, 1754−1762.
19. Harrigan, P. R., Stone, C., Griffin, P., Najera, I., Bloor, S., Kemp, S., Tisdale, M., and Larder, B. (2000) *J. Infect. Dis. 181*, 912−920.
20. Miller, V., Ait-Khaled, M., Stone, C., Griffin, P., Mesogiti, D., Cutrell, A., Harrigan, R., Staszewski, S., Katlama, C., Pearce, G., and Tisdale, M. (2000) *AIDS 14*, 163−171.
21. Schinazi, R. F., Lloyd, R. M., Jr., Nguyen, M. H., Cannon, D. L., McMillan, A., Ilksoy, N., Chu, C. K., Liotta, D. C., Bazmi, H. Z., and Mellors, J. W. (1993) *Antimicrob. Agents Chemother. 37*, 875−881.
22. Schuurman, R., Nijhuis, M., van Leeuwen, R., Schipper, P., Collis, P., Danner, S. A., Mulder, J., Loveday, C., Christopherson, C., Kwok, S., Sninsky, J., and Boucher, C. A. B. (1995) *J. Infect. Dis. 171*, 1411−1419.
23. Feng, J. Y., and Anderson, K. S. (1999) *Biochemistry 38*, 9440−9448.
24. Orr, D. C., Figueiredo, H. T., Mo, C. L., Penn, C. R., and Cameron, J. M. (1992) *J. Biol. Chem. 267*, 4177−4182.
25. Kati, W. M., Johnson, K. A., Jerva, L. F., and Anderson, K. S. (1992) *J. Biol. Chem. 267*, 25988−25997.
26. Rittinger, K., Divita, G., and Goody, R. S. (1995) *Proc. Natl. Acad. Sci. U.S.A. 92*, 8046−8049.
27. Kool, E. T. (1998) *Biopolymers 48*, 3−17.
28. Ray, A. S., and Anderson, K. S. (2001) *Nucleosides, Nucleotides Nucleic Acids 20*, 1247−1250.
29. Kerr, S. G., and Anderson, K. S. (1997) *Biochemistry 36*, 14064−14070.
30. Feng, J. Y., and Anderson, K. S. (1999) *Biochemistry 38*, 55−63.
31. Feng, J. Y., Shi, J., Schinazi, R. F., and Anderson, K. S. (1999) *FASEB J. 13*, 1511−1517.
32. Furman, P. A., Jeffrey, J., Kiefer, L. L., Feng, J. Y., Anderson, K. S., Borroto-Esoda, K., Hill, E., Copeland, W. C., Chu, C. K., Sommadossi, J. P., Liberman, I., Schinazi, R. F., and Painter, G. R. (2001) *Antimicrob. Agents Chemother. 45*, 158−165.
33. Vaccaro, J. A., and Anderson, K. S. (1998) *Biochemistry 37*, 14189−14194.
34. Vaccaro, J. A., Parnell, K. M., Terezakis, S. A., and Anderson, K. S. (1999) *Antimicrob. Agents Chemother. 44*, 217−221.
35. Furman, P. A., Painter, G. R., and Anderson, K. S. (2000) *Curr. Pharm. Des. 6*, 547−567.
36. Kerr, S. G., and Anderson, K. S. (1997) *Biochemistry 36*, 14056−14063.
37. Chu, C. K., Schinazi, R. F., Arnold, B. H., Cannon, D. L., Doboszewski, B., Bhadti, V. B., and Gu, Z. (1988) *Biochem. Pharmacol. 37*, 3543−3548.
38. Thrall, S. H., Krebs, R., Wohrl, B. M., Cellai, L., Goody, R. S., and Restle, T. (1998) *Biochemistry 37*, 13349−13358.
39. Wohrl, B. M., Krebs, R., Goody, R. S., and Restle, T. (1999) *J. Mol. Biol. 292*, 333−344.
40. Hsieh, J. C., Zinnen, S., and Modrich, P. (1993) *J. Biol. Chem. 268*, 24607−24613.
41. Skoog, D. A., and Leary, J. J. (1992) *Principles of instrumental analysis*, 4th ed., Saunders Collge Publishing, New York.
42. Reardon, J. E., Furfine, E. S., and Cheng, N. (1991) *J. Biol. Chem. 266*, 14128−14134.
43. Patel, S. S., Wong, I., and Johnson, K. A. (1991) *Biochemistry 30*, 511−525.
44. Johnson, K. A. (1993) *Annu. Rev. Biochem. 62*, 685−713.
45. Arts, E. J., and Wainberg, M. A. (1994) *Antimicrob. Agents Chemother. 38*, 1008−1016.
46. Klarmann, G. J., Smith, R. A., Schinazi, R. F., North, T. W., and Preston, B. D. (2000) *J. Biol. Chem. 275*, 359−366.
47. Mickle, T., and Nair, V. (1999) *Bioorg. Med. Chem. Lett. 9*, 1963−1968.
48. Parker, W. B., White, E. L., Shaddix, S. C., Ross, L. J., Shannon, W. M., and Secrist, J. A. (1992) *Antiviral Res. 49*, 325−332.
49. Shannon, W. M. (1990) in *Advances in Chemotherapy of AIDS* (Diasio, R. B., and Sommadossi, J.-P., Eds.) pp 75−95, Pergamon, New York.

50. Back, N. K. T., Nijhui, M., Keulen, W., Boucher, C. A. B., Oude Essink, B. B., van Kuilenburg, A. B. P., van Gennip, A. H., and Berkhout, B. (1996) *EMBO J. 15*, 4040−4049.

51. Selmi, B., Boretto, J., Navarro, J. M., Sire, J., Longhi, S., Guerreiro, C., Mulard, L., Sarfati, S., and Canard, B. (2001) *J. Biol. Chem. 276*, 13965−13974.

52. Hurst, M., and Noble, S. (1999) *Drugs 58*, 919−949.

53. Ding, J., Das, K., Hsiou, Y., Sarafianos, S. G., Clark, A. D., Jr., Jacobo-Molina, A., Tantillo, C., Hughes, S. H., and Arnold, E. (1998) *J. Mol. Biol. 284*, 1095−1111.

54. Huang, H., Verdine, G. L., Chopra, R., and Harrison, S. C. (1998) *Science 282*, 1669−1675.

55. Doublie, S., Tabor, S., Long, A. M., Richardson, C. C., and Ellenberger, T. (1998) *Nature 391*, 251−258.

56. Franklin, M. C., Wang, J., and Steitz, T. A. (2001) *Cell 105*, 657−667.

57. Li, Y., Kong, Y., Korolev, S., and Waksman, G. (1998) *Protein Sci. 7*, 1116−1123.

58. Li, Y., and Waksman, G. (2001) *Protein Sci. 10*, 1225−1233.

59. Pelletier, H., Sawaya, M. R., Kumar, A., Wilson, S. H., and Josegh, K. (1994) *Science 264*, 1891−1903.

60. Sawaya, M. R., Prasad, R., Wilson, S. H., Kraut, J., and Pelletier, H. (1997) *Biochemistry 36*, 11205−11215.

61. Kulaeva, O. I., Koonin, E. V., McDonald, J. P., Randall, S. K., Rabinovich, N., Connaughton, J. F., Levine, A. S., and Woodgate, R. (1996) *Mutat. Res. 357*, 245−253.

62. Zhou, B., Pata, J. D., and Steitz, T. A. (2001) *Mol. Cell 8*, 427−437.

63. Patel, P. H., Suzuki, M., Adman, E., Shinkai, A., and Loeb, L. A. (2001) *J. Mol. Biol. 308*, 823−837.

64. Gao, H. Q., Boyer, P. L., Sarafianos, S. G., Arnold, E., and Hughes, S. H. (2000) *J. Mol. Biol. 300*, 403−418.

65. Boyer, P. L., and Hughes, S. H. (2000) *J. Virol. 74*, 6494−6500.

66. Harte, W. E., Jr., Starrett, J. E., Jr., Martin, J. C., and Mansuri, M. M. (1991) *Biochem. Biophys. Res. Commun. 175*, 298−304.

67. Marrone, T. J., Straatsma, T. P., Briggs, J. M., Wilson, D. K., Quiocho, F. A., and McCammon, J. A. (1996) *J. Med. Chem. 39*, 277−284.

68. Ford, H., Jr., Dai, F., Mu, L., Siddiqui, M. A., Nicklaus, M. C., Anderson, L., Marquez, V. E., and Barchi, J. J., Jr. (2000) *Biochemistry 39*, 2581−2592.

69. Lacey, S. F., and Larder, B. A. (1994) *Antimicrob. Agents Chemother. 38*, 1428−1432.

70. Lin, P. F., Gonzalez, C. J., Griffith, B., Friedland, G., Calvez, V., Ferchal, F., Schinazi, R. F., Shepp, D. H., Ashraf, A. B., Wainberg, M. A., Soriano, V., Mellors, J. W., and Colonno, R. J. (1999) *Antiviral Ther. 4*, 21−28.

71. Ray, A. S., Zhenjun, J., Chu, C. K., and Anderson, K. S. (2002) *Antimicrob. Agents Chemother. 46*, 887−891.

72. Esnouf, R. M. (1997) *J. Mol. Graphics Modell. 15*, 132−134, 112−113.

73. Merritt, E. A., and Murphy, M. E. P. (1994) *Acta Crystallogr. D50*, 869−873.

BI0121858